



HAL
open science

High temperature machine: Characterization of materials for the electrical insulation

Jean-Philippe Lecointe, Stéphane Duchesne, Dorin Cozonac, Gabriel Vélú,
Krzysztof Komez

► **To cite this version:**

Jean-Philippe Lecointe, Stéphane Duchesne, Dorin Cozonac, Gabriel Vélú, Krzysztof Komez. High temperature machine: Characterization of materials for the electrical insulation. *Open Physics*, 2020, 18 (1), pp.674-682. 10.1515/phys-2020-0109 . hal-03667497

HAL Id: hal-03667497

<https://hal.science/hal-03667497>

Submitted on 18 May 2022

HAL is a multi-disciplinary open access archive for the deposit and dissemination of scientific research documents, whether they are published or not. The documents may come from teaching and research institutions in France or abroad, or from public or private research centers.

L'archive ouverte pluridisciplinaire **HAL**, est destinée au dépôt et à la diffusion de documents scientifiques de niveau recherche, publiés ou non, émanant des établissements d'enseignement et de recherche français ou étrangers, des laboratoires publics ou privés.

Research Article

Jean-Philippe Lecoïnte, Stéphane Duchesne*, Dorin Cozonac, Gabriel Vêlu, and Krzysztof Komezà

High temperature machine: Characterization of materials for the electrical insulation

<https://doi.org/10.1515/phys-2020-0109>

received March 31, 2020; accepted May 31, 2020

Abstract: This paper aims to present and analyze the materials adapted to design a machine that can work with a high current density without any specific cooling system. In other words, the machine is equipped with material that supports high internal temperature, about 500°C. Candidate materials are selected and the authors indicate that inorganic insulation should be preferred for conductors and slot insulations. Tests are carried out on material selection through measurement of the turn-to-turn voltage, insulation resistances, and the parallel capacitances.

Keywords: motor insulation, ceramics cements, AC motors, high temperature environment

1 Introduction

Nowadays, in an electrical rotating machine, the winding temperature is the main limiting parameter in terms of power to weight ratio since the usual working temperature, which cannot exceed 240°C, is linked to the organic conductor insulation [1]. However, some applications need electrical machines beyond the usual thermal limit, in high temperature (HT) environment, for example, in the domains of furnaces smoke extractors, in spatial applications, or in nuclear industry [2–4].

Improving the working temperature, either for HT applications or for machines with high current densities,

requires all the electrical machine components to be made with specific materials that can work with a high internal temperature. Increasing the temperature does not only depend on the insulation conductor. The major effects over 250°C are the metal corrosion and the thermal decomposition of organic materials [1,5,6]. The slot insulation, the ball-bearings, or the plastic parts such as the fan or the connection plate in the terminal box must be strong enough to resist at higher temperatures. The magnetic circuit should also be able to work magnetically at HT.

The objective of this work is to design a three-phase induction machine powered by a balanced sinusoidal system with an internal temperature in a range 400–500°C. Consequently, in the first part of this paper, the reasons that motivated the authors to design an induction machine are discussed. The second part analyses a copper plated wire with a thin ceramic insulation, which is dedicated to HT. The authors compare it to a more classical mica-taped wire which has a thicker insulation, not easy to use in an electric machine. The wire characteristics are also compared with those typically observed for typical copper wires with organic insulation. The third part focuses on the slot insulation. All the materials characterized are commercially available and the tests have been performed under atmospheric conditions with a temperature range between 20 and 500°C.

2 HT constraints

2.1 Parameters restricting the temperature increase in a conventional electric motor

In order to reach a maximum of 500°C within a machine, it is essential to significantly overcome the limits of conventional machines. The evaluation of the weak points, occurring with temperature increase, can be done

* Corresponding author: Stéphane Duchesne, Univ. Artois, UR 4025, Laboratoire Systèmes Electrotechniques et Environnement (LSEE), Béthune, F-62400, France, e-mail: stephane.duchesne@univ-artois.fr

Jean-Philippe Lecoïnte, Dorin Cozonac, Gabriel Vêlu: Univ. Artois, UR 4025, Laboratoire Systèmes Electrotechniques et Environnement (LSEE), Béthune, F-62400, France

Krzysztof Komezà: Institute of Mechatronics and Information Systems, Technical University of Lodz, Stefanowskiego 18/22, 90-924, Lodz, Poland

by dividing the machine components into five families of elements analysed below:

- The magnetic circuit. The magnetic circuit of electric machines, to limit the eddy current, is traditionally made up of a stack of electric steel sheets. They are usually made of an alloy of iron (Fe) and silicon (Si) covered with a thin insulation layer ($\approx \mu\text{m}$). The curie temperature of these kinds of alloys reach 700°C and several studies show that magnetic characteristics decrease with temperature but remain exploitable in the targeted range [7]. The problem is more sensitive for the insulation layer, depending on the selected sheets. Traditionally, non-oriented grains sheets are isolated using organic materials added at the end of manufacture. On the other hand, anisotropic (grain-oriented) sheets have a phosphate based inorganic insulating layer that is naturally formed during the process. These sheets are capable of operating at HTs while retaining magnetic characteristics, which are of interest for the electrical machine. Nevertheless, their anisotropy requires a subtle assembly of the magnetic circuit [8]. FeNi laminations are also well fitted to HTs but the cost limits greatly a large use of this material [9,10].
- The electrical conductors. Usually, conductors are made with copper whose resistivity increases with temperature. Copper can be used at HT but other metal alloys can bring better performance at HT like silver–palladium alloys (AgPd). Moreover, at HT, the oxidation mechanism of copper [6,11] requires to cover the main conductor with metals such as nickel or materials stable at high temperatures [12]. In addition, it is essential to find a suitable solution to ensure the electrical link between the coils. The classical process uses alloys of lead and tin (PbSn) that are unable to work beyond 300°C . Other solutions, based on silver or aluminium alloys, for example, can be used [13,14].
- The electrical insulation of the wire. Organic polymer such as polyamide-imide and polyester-imide (PAI/PEI) are often used but they cannot work over 200°C . Polymer materials such as polyimide (PI), Teflon AF (PTFE), or PEEK, can work up to 250°C and probably higher but the use of these materials for wire insulation is still experimental [15,16]. Another solution would be to use materials with a low percentage of nanoparticles but, for the moment, commercially available products are designed to extend the life of insulation in the event of partial discharges (corona-resistant wires) [17]. All these temperature limits are defined according to the thermal class that defines an operating time of 20,000 standard hours. Exceeding these standardized temperatures leads to a reduction of the lifetime following the Arrhenius law since organic materials are considered.
- Magnets. Permanent magnets are not known for their ability to heat up. Samarium/cobalt alloys (Sm/Co) are the most efficient varieties in this respect. However, their operating range remains limited to 350°C . Beyond that, they irreversibly lose their magnetic property [20,21].
- Auxiliary components such as the fan or the connector board. Usually made of consumer polymers such as PET, with a maximum of 120°C , although these can be replaced quite easily by steel components offering higher thermal capacities.
- The bearings. The classical bearings should be replaced at HT. The solution is to use ceramic or partial ceramic bearings. The bearings are able to operate in a range of temperature up to 450°C ; they include a treatment of steel parts with manganese–phosphate and ceramics, which make them resistant to heat. The organic lubricant is replaced by solid lubricants such as molybdenum disulphide coating (MoS_2) for temperature up to 500°C or tungsten disulphide (WS_2) beyond and up to 650°C [18,19].

This quick review shows that the main weakness of the electrical machine with respect to temperature is the electrical insulation system, including the insulating layer of the wires, the sheets placed at the bottom of the slots and those separating the magnetic laminations. Polymers are most often used because their mechanical properties are particularly well suited to the winding process of the machine. Inorganic materials such as mica, ceramics, and fibreglass are nowadays the best candidates for a significant temperature increase in machines. However, their poor mechanical properties make the coil wound operations much more hazardous and it is necessary to define new winding methods for these machines based on a thorough understanding of these materials.

2.2 Selection of topology for the prototype

Taking into account the observations made in the previous part, the machine choice can be done. With a specification claimant, an internal temperature reaching 500°C , the use of permanent magnet is impossible. In addition, considering the limited insulation capabilities of the inorganic material, we have chosen the motor that can operate without an inverter to reduce the stresses on the insulation layers due to voltage fronts [22]. The induction machine is therefore the natural choice considering these assumptions. The rotor is simple to build with an aluminum or a copper cage.

3 Winding wires for high temperature

3.1 HT wire technologies

Conventional organic polymers could not work over 280°C. Thus, it is necessary to use non-organic materials that resist much higher to heat [23]. Inorganic material family includes materials partly or fully crystalline obtained by vitrification or sintering operation. For electrical insulation, the most used materials are oxides such as aluminum oxide (Al_2O_3), silicon dioxide (SiO_2), magnesium oxide (MgO), lead oxide (PbO), titanium dioxide (TiO_2), barium titanate (BaTiO_3), or mica [24,25]. Their good insulation characteristics and poor mechanical capacities, especially in traction, make them unsuitable for use in windings.

Some commercial references for ceramic-insulated wires already exist [26–29]. These wires are used in extremely harsh conditions (to supply sensors located in nuclear power plants, for example). During their manufacturing process, the insulation layer cannot be manufactured by traditional sintering. It is necessary to use alternative techniques such as vapor deposition, plasma spraying, or flame spraying of a ceramic powder on the metal. This affects the uniformity of the coated layer. The obtained wires have an insulating layer made of a rather uneven agglomerate of micro-particles that give rise to significant porosities. This perturbed surface state is responsible for the appearance of a discharge phenomenon even at low voltage [30].

To evaluate the possibilities of using these ceramic insulators in an electrical machine, the authors have characterized two wires. First, denoted as Wire A, is a ceramic-coated wire available with a diameter of 0.518 mm and made with a heart of Cu (73% of the weight) and Ni-plated layer (27%). The insulation layer of 9 μm thickness is made of ceramic mainly composed of Al_2O_3 and SiO_2 . Second, denoted as Wire B, is a mica-fiberglass taped wires of 0.7 mm diameter made of Nickel-plated copper (in the same proportions as the previous one) taped with a thin film of mica phlogopite and fiberglass (thickness of 100 μm). This second wire has an insulating layer 10 times thicker than Wire A, which will negatively impact the slot fill rate.

The next step is to analyze the critical bending radius, the parallel resistance R_p , the parallel capacitance C_p , the loss insulation $\tan \delta$, the PDIV, the breakdown voltage U_b , and the conductor resistivity r .

3.2 Bending radius of inorganic insulation

Wires insulated with inorganic materials are too fragile to be handled as usual. The wire curvature is therefore a critical parameter; the manufacturers specify an R_b critical bending radius beyond which the insulation layer is damaged. R_b depends on the wire diameter D_c ($R_b = 10D_c$ for Wire A). Even if the radius problem is less critical for taped wires such as Wire B, the same tests have been carried out. The CEI 60,851 standard presents two devices for the insulation test of enameled wires: twisted pair and winding around a cylinder. The second one has been chosen to better control the applied stress. Both wires are therefore wrapped under different cylinders with D_c diameters ranging between $5D_c$ and $50D_c$. The surfaces of stressed wires are analyzed with a microscope, as shown in Figure 1. Tests are then conducted by placing the wires in metal alloys (SnPb) melted and kept in a liquid state at 350°C. This temperature is far below the limits of the tested wires. The short-circuits between melted metal and main conductor of the wires are measured and the results are presented in Table 1.

The tests are done using four different diameters of Wire A: 0.3, 0.5, 0.8 and 1 mm. The Wire B with 0.7 mm diameter is also analyzed.

- The Figure 1a shows the non-stressed ceramic insulation on the conductor. For a $50D_c$ radius, cracks are observed in Figure 1b but their sizes are the lowest compared with other diameters.
- Between $20D_c$ and $30D_c$ (Figure 1c), the ceramic surface is easily fractured but the fissures remain too narrow to let pass the melted liquid up to the conductor. This effect explains the AC behavior of the ceramics wires since the insulation is fissured and damaged. The visual observation shows that detachments of the ceramic grains and bleaching of the surface appear for bending radius lower than $20D_c$.
- It is observed that, up to $20D_c$, the ceramic insulation (8 to 10 μm) is seriously damaged. Indeed, the wire bending during the winding process imposes compression stresses on one side and tensile stress on the other side. On the external radius, the cracks are widened and on the internal radius, they are narrowed. As a result, the insulation layer becomes very porous on the external side and the real thickness of this layer is reduced.

The Wire B tests show that no short-circuit occurs for all the samples. The insulation has, for all tested diameters, local damages of fiberglass tape but the conductor is still isolated.

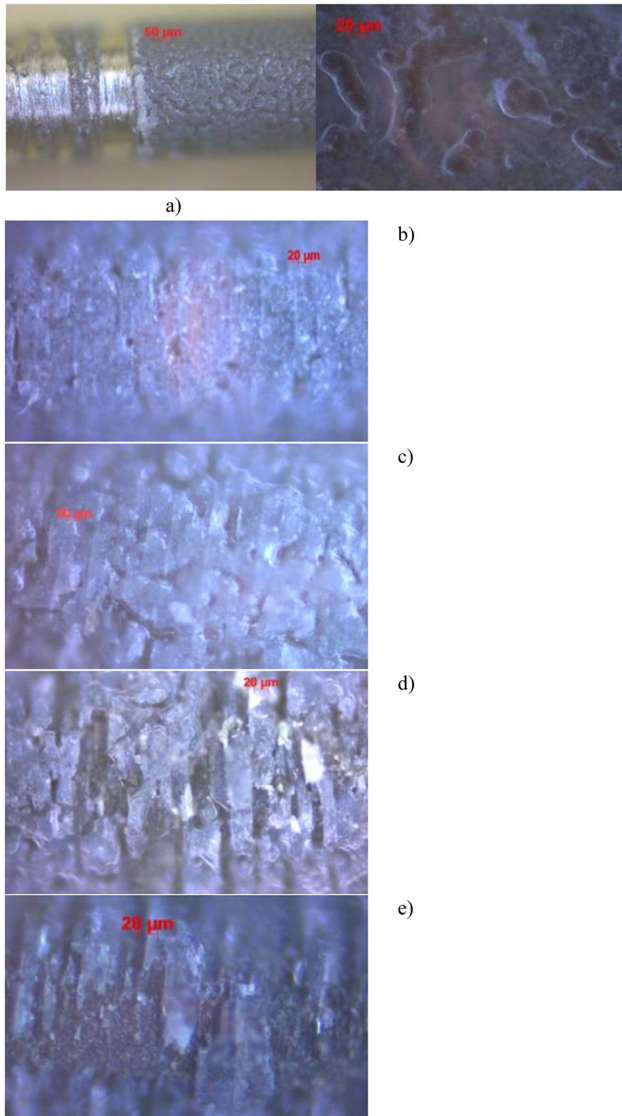


Figure 1: Surfaces of ceramic-coated Wire A wrapped with different bend radius. (a) Ceramic surface state non-stressed, (b) ceramic surface after $50D_c$, (c) ceramic surface after $30D_c$, (d) ceramic surface after $15D_c$, (e) ceramic surface after $5D_c$.

This part of the study showed that the bending radius problem is critical for Wire A but not for Wire B. However, it should be remembered that Wire B has a thicker insulating layer.

3.3 Electrical and breakdown strength

Measuring the permittivity, the leakage current, the dielectric losses represented by the factor $\tan \delta$ and the breakdown voltage U_b makes it possible to identify the dielectric characteristics of ceramics. The typical voltage–current curve of ceramic insulation gives the range of use in the zone close to the breakdown voltage [31]. Measurements of electrical discharges are presented in Figure 2a and b for Wires A and B, respectively. It shows that individual PD pulses appear for Wire A at low voltages (215 V). They differ slightly from the usual “breakdown voltages”. The initiation of the conduction channel during the breakdown phase can be the cause of the occurrence of discharges at such low-voltage levels; an increase of electronic mobility in the insulation layer will inevitably have an impact on the dielectric constant and the insulation resistance [31]. The external surface of the insulation layer is non-regular, which leads to many phenomena of discharges at the surface.

The discharge inception voltage for Wire A and the first PD observed for Wire B has been measured when the temperature is increased, as shown in Figure 3. The voltage is progressively increased until the first discharges are observed. The occurrence of PD is not a relevant health indicator for ceramic insulation due to the several factors that can influence the structure of the insulation, independent of each other (porosity, cracks, moisture, etc.) and cause strong variations of the PDIV. Therefore, a breakdown test is also necessary. In the temperature range from 400 to 500°C, the variation of the breakdown voltage and

Table 1: Results of ceramic and mica insulated wires during mandrel test

Wire diameter		$D_c = 0.3 \text{ Mm}$	$D_c = 0.5 \text{ mm}$	$D_c = 0.7 \text{ Mm}$	$D_c = 0.8 \text{ mm}$	$D_c = 1 \text{ mm}$
Wire		A	A	B	A	A
Mandrel diameter	$5D_c$	×	×	√	×	×
	$10D_c$	×	×	√	×	×
	$15D_c$	×	×	√	×	×
	$20D_c$	√	√	√	√	√
	$25D_c$	√	√	√	√	√
	$30D_c$	√	√	√	√	√
	$50D_c$	√	√	√	√	√
No stress		√	√	√	√	√

× short-circuit; √ short-circuit not detected.

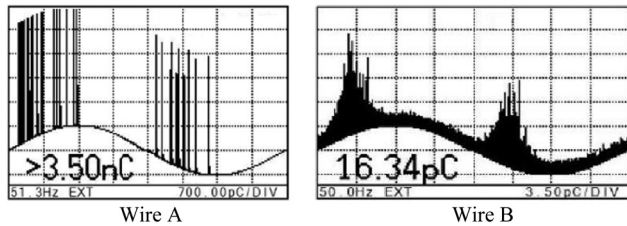


Figure 2: Inception of discharge and quantity of charges observed with AC voltage. Wire A – ceramic coated; Wire B – mica-fiberglass.

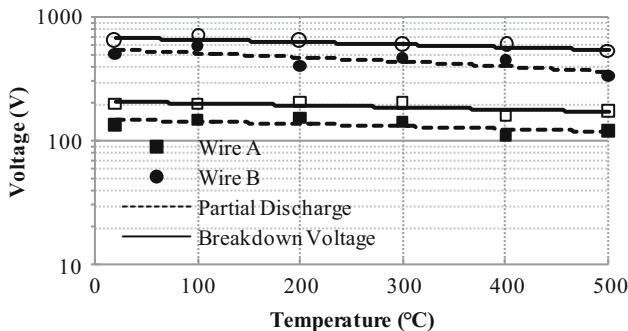


Figure 3: Regression curves of the temperature impact on the first DP and breakdown voltages. Test made with a tube of diameter $20D_c$ and supplied by a 50 Hz sinusoidal AC source.

the variation of the voltage corresponding to the phenomena discharge are the same. The gap between the two phenomena is quite constant. The levels for Wire B are higher than those for Wire A.

Then, the variation of the parallel resistance R_p between the conductor wire and the cylinder with the temperature is shown in Figure 4. Each point results from an average of measurements made on 11 individual samples. The insulation resistance R_p provides feedback on the variation of the leakage current at a specified voltage.

3.4 Conductor resistance variation

Copper and nickel are the main material for a wire used in HT. Conductors of 1 m length of each type of wire were placed in an oven and the values of relative resistance r were measured. As the temperature rises, the conductor resistivity increases compared with 20°C value as shown in Figure 5.

3.5 Discharge phenomenon

The measurement of the partial discharge occurring on Wire B at HT is shown in Figure 2b. A sinusoidal voltage

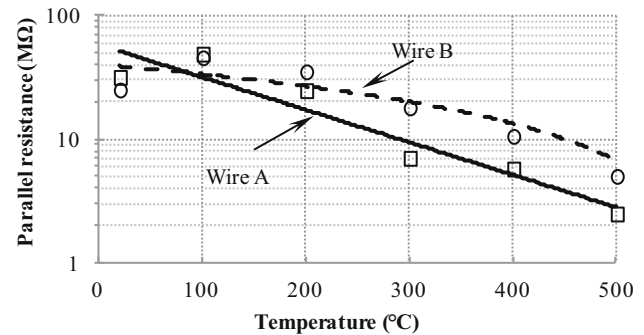


Figure 4: Variation of the parallel resistance R_p with the temperature.

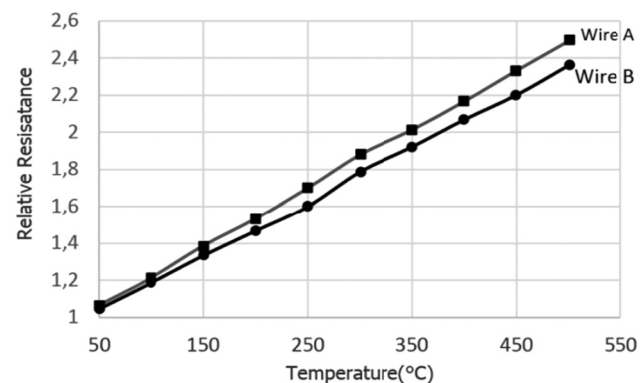


Figure 5: Variation of Wire A (ceramic coated) and B (mica-fiberglass) resistance with the temperature.

U_{rms} is applied and the amount of electrical charge passing through the insulation is measured. The measurement made on Wire B (Figure 2a) is analogous to the discharge pattern of conventional organic insulation wires. The initiation of low-voltage discharges is a special case of Wire A, very energetic discharges pass through the insulation layer. The low levels of discharge initiation voltages can be explained by the occurrence of rather high local electric fields, which are caused by the high permittivity – especially in a high-temperature environment – and more significantly by the high heterogeneity of the ceramic insulation layer. The porosity of the ceramic can lead to the appearance of shorts in the cavities, which form plasma channels responsible for the breakdown.

3.6 Summary of the properties of the wires

The characteristics of the tested wires at 500°C are summarized in Table 2. Both Wire A and Wire B have

Table 2: Comparison of the studied wires at 500°C

Parameter	Bending radius	R_p (M Ω)	C_p (pF)	$\tan \delta$	r ($\times r_{20^\circ\text{C}}$)	PDIV (V)	U_{break} (V)
Wire A	$20D_c$	2.47	68.6	0.099	2.38	119	173
Wire B	—	1.74	57.3	0.206	2.43	328	540

good thermal stability in terms of dielectric parameters. Partial discharge onset voltage and breakdown voltages for Wire A appear between 120 and 180 V in the 400–500°C range. Under the same conditions, Wire B has better characteristics for each parameter. These two wires may be good candidates for an electrical machine operating at 400–500°C, with a slight advantage for Wire B.

This section assessed the limitations of the two wires technologies. It showed a slightly better dielectric and mechanical behavior for Wire B. However, it also pointed out that, with the right precautions, it is possible to use Wire A, which has finer insulation, for winding electrical machines.

4 Insulation slot and impregnation solution

4.1 Slot insulation

The most common Class C material for slot insulation is Nomex[®]-Kapton[®]-Nomex[®] laminated composite. Certain associations of fiberglass, polyimide, or Nomex[®] with silicone resins are also possible. However, their NOMEX properties decrease with increasing temperature slightly in nitrogen and drastically in air [32]. Other solutions such as mica-taped or ceramic as paper or woven tape can be selected for slot insulation. They generally have excellent thermal stability up to 1,300°C making them suitable for the intended application if we can accommodate their shortcomings:

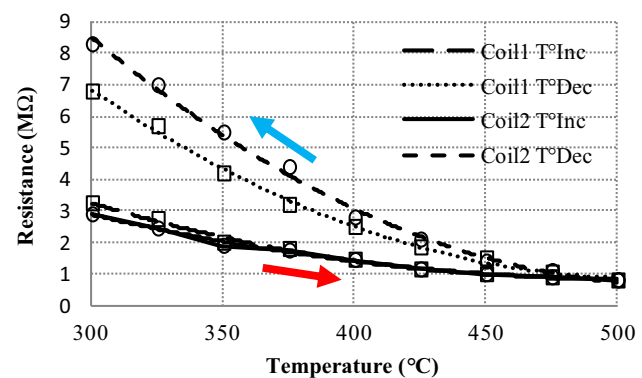
- the relative mechanical weakness of the mica makes it necessary to use a fiberglass mesh to hold it inside the slot;
- ceramic paper requires impregnation – preferably mineral – for the same reasons.

The ceramic cloth is similar to a fiberglass, but with a lower degradation with the temperature increase. This material can be interesting to use, since after impregnation process, the whole system reacts as a composite

material composed of the ceramics cloth and the mineral cement. In that case, the interweaving of ceramic fibers tends to trap air bubbles during the impregnation process. The obtained result has lower performances as expected due to these porosities and the insulation capabilities remain poor.

Insulation resistance measurements were carried out on two ceramic coils. A mica-fibreglass composite tape (thickness 90 μm) was placed between the iron core and the winding. Two mica sheets of 250 μm provide lateral protection. The resistance between the wire strand and the iron core is measured for different temperatures at 10 kHz with an Agilent 4,284 A impedance analyzer that works with small signals (2 VRMS sinusoidal voltage). The temperature was stabilized for 20 min before each measurement was recorded.

The variations of the insulation resistance are presented in Figure 6 between 300°C and 500°C. Two coils (one and two) have been tested in an oven by measuring the parameters during a cycle of temperature rise and then fall. This figure shows, first of all, a low dispersion between the results obtained with the two coils. In addition, it shows a significant increase in the resistance during the temperature decrease. It can be assumed that, during the first phase, the cement reacts with heat treatment. In reality, the cement hardening is a very long reaction which can hold out during several

**Figure 6:** Insulation resistance of the slot insulation (mica-fibreglass tape).

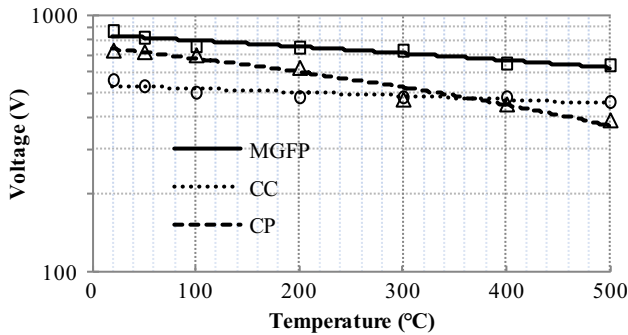


Figure 7: Regression curves of the temperature impact on the first DP for inorganic insulation.

weeks before the stabilization of its properties. The heat treatment tends to improve the capabilities of the impregnation by acceleration of the natural hardening process. Additional studies will be needed to understand and predict the properties of a whole insulation system using these materials.

The use of such slot insulation means that the coils are rigid. This presents a problem when inserting them into the slot of a traditional machine, even with open slots. The final coil cannot be bent or the insulation will be damaged.

PD tests with temperature variation are performed at 50 Hz for three slotted insulation candidate: mica glass fiber insulation, ceramic cloth (CC) and ceramic paper (CP). The results are shown in Figure 7. These tests show that mica paper is the most appropriate candidate for slot insulation at HT. Its mechanical and electrical properties up to 500°C are good enough for the intended application. CC and CP are rather options for reinforcing the border of coils during the ceramic impregnation.

4.2 Impregnation cement

The best way for the impregnation is to use cement directly on the coils. The role of this cement is not only to encapsulate the coil to protect it from external influences. The weak performance of the tested wires requires that it improves the inter-turn insulation as would a conventional impregnation resin. Cement results from a chemical reaction compatible with a vacuum and pressure conventional process. Figure 8 shows a coil impregnated with ceramic cement.

Wire A has been analyzed by using three types of impregnation. The first cement called type A has a grain size of $1/20 \mu\text{m}$, a thermal conductivity of $1.7 \text{ Wm}^{-1} \text{ K}^{-1}$, and a good bonding strength. The second cement called

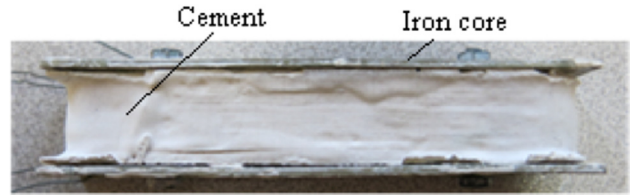


Figure 8: Winding coil impregnated with ceramic cement.

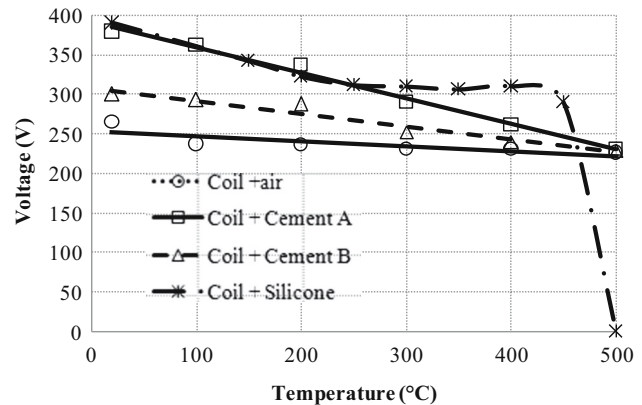


Figure 9: Impact of temperature on PD behavior for ceramic insulated coils with various impregnation types.

type B has a grain size of $1/40 \mu\text{m}$, a thermal conductivity of $5.72 \text{ Wm}^{-1} \text{ K}^{-1}$, and a very good bonding strength. The third one is high-temperature silicone resin. Both cement types are selected for their properties: lowest grains size, highest dielectric strength, highest thermal conductivity and expansion, good bonding properties, and lowest mass density. Tests are done on the circular miniaturized coils taking into account the admissible bend radius deduced in previous tests. The variations of the PDIV with the temperature are shown in Figure 9.

The results show that the cement impregnation can improve the insulation capabilities of the coil, slightly for the cement B and more strongly for the cement A. Moreover, the properties of the two cements decrease with the increase in temperature between 400 and 500°C, the influence of impregnation becomes insignificant compared with non-impregnated coils. So, it is possible to admit that ceramic impregnation may be used just for mechanical properties of the final coil.

5 Conclusion

This paper proposes a characterization of insulation materials, which can be used to build HT induction

machine. The authors characterized the wire and slot insulation and the impregnation solutions by selecting, for each insulation level, different candidate materials commercially available. Based on the particular properties of these materials, the study led to fix the geometry of the coils that are imposed by the use of rigid ceramic insulation solutions. The friability of the mica tape insulation after 400–500°C and the reduction in the gap-filling factor caused by the greater thickness of the wire insulation, make it suitable for the use of Wire B compared to Wire A, especially for large machines. The study also demonstrated that it was possible to use a ceramic-based cement for the impregnation of the winding. Thus, the technology described in this study is dedicated to grid-connected induction machines. The use of a PWM power supply will require to take into account some additional stress on the insulation, which will probably imply a lower voltage supply.

A complementary work will concern the magnetic material and the design of the induction machine [33].

Acknowledgments: This work has been achieved within the framework of CE2I project (Convertisseur d’Energie Intégré Intelligent). CE2I is co-financed by European Union with the financial support of European Regional Development Fund (ERDF), French State, and the French Region of Hauts-de-France.

References

- [1] Aymonino F, Lebey T, Malec D, Petit C, Michel JS, Anton A. Dielectrics measurements of rotating machines insulation at high temperature (200–400°C). *Proc IEEE CEIDP Conf.* 2006;740–3. doi: 10.1109/CEIDP.2006.312038.
- [2] Roger D, Iosif V, Duchesne S. High temperature motors: investigations on the voltage distribution in windings at a short scale times for a PWM supply. *Proc IEEE IEMDC.* 2017. p. 1–7. doi: 10.1109/IEMDC.2017.8002179.
- [3] Roopnarine, Motor for high temperature application, US Patent (2011), US8581452B2.
- [4] Peralta P, Wellerdieck T, Steinert D, Nussbaumer T, Kolar J. Ultra-high temperature (250°C) bearingless permanent magnet pump for aggressive fluids. *IEEE/ASME Trans Mechatron.* 2017;22(5):2392–4. doi: 10.1109/TMECH.2017.2729618.
- [5] Kakuta T, Sekiguchi N, Horikoshi S, Yatsuhashi M, Sunazuka H, Fujiwara M. Heat and radiation resistant cable for the use on LMFB. *IEEE Trans Nucl Sci.* 1982;29:695–9. doi: 10.1109/TNS.1982.4335939.
- [6] Zhu Y, Mimura K, Isshiki M. Oxidation mechanism of copper at 623–1073 K. *Mat Trans.* 2002;43(9):2173–6. doi: 10.2320/matertrans.43.2173.
- [7] Ababsa ML, Ninet O, Velu G, Lecoite JP. High-temperature magnetic characterization using an adapted Epstein frame. *IEEE Trans Magn.* 2018;54(6). doi: 10.1109/TMAG.2018.2811727.
- [8] Cassoret B, Lopez S, Brudny JF, Belgrand T. Non-segmented grain oriented steel in induction machines. *PIER-C.* 2014;47:1–10. doi: 10.2528/PIERC13112007.
- [9] Lu X, Xu Y-b, Fang F, Zhang Y-x, Wang Y, Jiao H-t, et al. Microstructure, texture and precipitate of grain-oriented 4.5 wt% Si steel by strip casting. *JMMM.* 2016;404:230–7. doi: 10.1016/j.jmmm.2015.12.043.
- [10] Qin J, Yang P, Mao W, Ye F. Effect of texture and grain size on the magnetic flux density and core loss of cold-rolled high silicon steel sheets. *JMMM.* 2015;393:537–43. doi: 10.1016/j.jmmm.2015.06.032.
- [11] Zhu Y, Mimura K, Lim JW, Isshiki M, Jiang Q. Brief review of oxidation kinetics of copper at 350°C to 1050°C. *Metall Mater Trans A.* 2006;37:1231–7. doi: 10.1007/s11661-006-1074-y.
- [12] Kalita G, Ayhan ME, Sharma S, Shinde SM, Ghimire D, Wakita K, et al. Low temperature deposited graphene by surface wave plasma CVD as effective oxidation resistive barrier. *Corros Sci.* 2014;78:183–7. doi: 10.1016/j.corsci.2013.09.013.
- [13] Kokash MZ, Sivasubramony RS, Then Cuevas JL, Zamudio AF, Borgesen P, Zinn AA, et al. Assessing the reliability of high temperature solder alternatives. *IEEE Proc ECTC Conf.* 2017;1987–95. doi: 10.1109/ECTC.2017.88.
- [14] Onuki J, Chiba A, Kawakami M, Tamahashi K, Sugawara Y, Inami T, et al. Highly reliable high-temperature superplastic Al-Zn eutectoid solder joining with stress relaxation characteristics for next generation SiC power semiconductor devices. *Proc ISPSD Conf.* 2017;495–8. doi: 10.23919/ISPSD.2017.7988887.
- [15] Aymonino F. Degradation and Dielectrics measurements of rotating machines insulation at high temperature (200–400°C). PhD thesis. Université Toulouse II-Paul Sabatier; 2007.
- [16] Hammoud AN, Baumann ED, Overton E, Myers IT, Suthar JL, Khachen W, et al. High temperature dielectric properties of Apical, Kapton, PEEK, Teflon AF, and Upilex polymers. *Proc IEEE CEIDP Conf.* 1992;549–54. doi: 10.1109/CEIDP.1992.283158.
- [17] Yin W, Flanagan K, Zhao R, Artus D, Sigler C, Jia X, et al. High temperature nanocomposite insulation for high power density machines. *Proc IEEE ICD Conf.* 2016;367–71. doi: 10.1109/ICD.2016.7547620.
- [18] <http://www.nsk.com/>. Bearings for High-Temperature Environments; 2014.
- [19] <http://traitements-preparations-moteurs.aquitaine-racing-service.fr/>. Disulfure de tungstène WS2; 2014.
- [20] Fingers RT, Rubertus CS. Application of high temperature magnetic materials. *IEEE Trans Magn.* 2000;36(5):3373–5. doi: 10.1109/20.908805
- [21] Raminosoa T, El-Refaie A, Torrey D, Grace K, Pan D, Grubic S, et al. Test results for a high temperature non-permanent-magnet traction motor. *IEEE Trans Ind Appl.* 2017;53(4):3496–504. doi: 10.1109/TIA.2017.2687870.
- [22] Mihaila V, Duchesne S, Roger D. A simulation method to predict the turn-to-turn voltage spikes in a PWM fed motor winding. *IEEE Trans Dielectr Electr Insul.* 2011;18(5):1609–15. doi: 10.1109/TDEI.2011.6032831.

- [23] Mark J-E. Physical properties of polymers handbook. New York: Springer; 2007.
- [24] Sakakibara T, Akagi M, Hashimoto Y, Haruta Y, Maeda T. High heat-resistant ceramic coating. Proc IEEE ICSD Conf. 2001;2001:199–201.
- [25] Mitsui H, Kumazawa R, Aizawa R, Okamoto T, Kanegami M. Investigation of the voltage life of mica-alumina composite insulation at high temperatures. Electr Eng Jpn 2001;129:199–201. doi: 10.1109/ICSD.2001.955590.
- [26] <http://www.cables-cgp.com>. Cerafil500. Ceramic insulated wire. Available: <http://www.cables-cgp.com>; 2014.
- [27] <http://www.ceramawire.com/>. Ceramawire. Ceramic insulated wire. Available: <http://www.ceramawire.com/>; 2014.
- [28] <http://www.schupp.ch>. KD 500 et KD 700 Ceramic insulated wire. Available: <http://www.schupp.ch>; 2014.
- [29] <http://www.vonroll.ch>, “SK 650, Mica taped wires,” ed: vonRoll; 2014.
- [30] Nikonov V, Bartnikas R, Wertheimer MR. The influence of dielectric surface charge distribution upon the partial discharge behavior in short air gaps. IEEE Plasma Sci. 2001;29(6):866–74. doi: 10.1109/27.974972.
- [31] Owate IO, Freer R. AC breakdown characteristics of ceramic materials. J Appl Phys. 1992;72:2418–22. doi: 10.1063/1.351586.
- [32] Dupont Technical Guide for NOMEX Brand Fiber,” 2001.
- [33] Cozonac D, Lecoïnte J-Ph, Duchesne S, Velu G. Materials characterization and geometry of a high temperature induction machine. Proc ICEM Conf. 2014:2499–505. doi: 10.1109/ICELMACH.2014.6960538.